


Article

Thermal Design and Experimental Validation of a Lightweight Microsatellite

Hongzhou Huang and Changgen Bu * 

School of Engineering and Technology, China University of Geosciences, Beijing 100084, China;
huanghongzhou@email.cugb.edu.cn

* Correspondence: bucg@cugb.edu.cn

Abstract: The multiple working modes, complex working conditions, frequent changes in external heat flux, and high-power consumption of satellites all pose great difficulties to their thermal design. In this paper, the material MB15 magnesium alloy was used, which has not been performed for the main structure of satellites. This material not only reduces the weight of the structure and the launch cost, but also its good thermal conductivity is very helpful for the thermal control design of the satellite. This paper mainly describes the design of a thermal control system for lightweight microsatellites. Firstly, the satellite structure, thermal control indices of the main equipment, and the power consumption of the equipment in different working modes are introduced. Then, the external heat fluxes are analyzed, the position of the heat dissipation surface and extreme conditions are confirmed, and detailed thermal designs of each part of the satellite are determined via the combination of active and passive thermal control. Finally, the thermal balance test is carried out for the whole satellite. It is found that the deviation between the temperature of the thermistor and thermocouple at the same moment in the thermal analysis simulation data and thermal balance test is generally within 0.5 °C, and the maximum difference is not more than 1.7 °C, which indicates that the simulation model is well established and that the thermal analysis is reliable.

Keywords: microsatellite; magnesium alloy; external heat flux; thermal balance test



Academic Editor: Hyun-Ung Oh

Received: 28 November 2024

Revised: 10 January 2025

Accepted: 13 January 2025

Published: 14 January 2025

Citation: Huang, H.; Bu, C. Thermal Design and Experimental Validation of a Lightweight Microsatellite. *Aerospace* **2025**, *12*, 52. <https://doi.org/10.3390/aerospace12010052>

Copyright: © 2025 by the authors. Licensee MDPI, Basel, Switzerland. This article is an open access article distributed under the terms and conditions of the Creative Commons Attribution (CC BY) license (<https://creativecommons.org/licenses/by/4.0/>).

1. Introduction

The purpose of the satellite thermal control subsystem is to control the temperature of the satellite components within the range of design indices based on the satellite platform [1] to ensure that the instruments, equipment, and institutions can work normally in the space environment. The satellite structure subsystem is an important part of the satellite [2], which is a functional component that carries and transmits force, provides space for the installation of payloads and instruments, ensures the strength and rigidity of the satellite, and is the basis of thermal control subsystems, whose design program directly affects the success or failure of the satellite launch. Satellite structure is the basis of thermal control design, and thermal control measures can be implemented based on the structure [3,4]. Therefore, in the structural design of the satellite platform, the thermal control design requirements should be considered from the aspects of material selection, configuration, etc., and while the satellite structure meets a certain degree of strength and stiffness to realize the load-bearing function [5–7], it should also have good heat transfer performance to meet the heat dissipation requirements of the satellite equipment [8,9].

Traditional satellites commonly use materials for aluminum and aluminum alloy. Aluminum alloy has high stiffness and strength, and good forming process performance and

corrosion resistance, good thermal conductivity, non-ferromagnetism, radiation resistance is better, but with the satellite structure of the lightweight and more demanding magnesium alloy materials as the 21st century, new green environmental protection structure materials, will be in the realization of the lightweight products in the field of technology to play a more and more important role in the role of the lightweight [10–13]. Role: magnesium alloy has high specific strength and specific stiffness, good dimensional stability, thermal and electrical conductivity, excellent casting, cutting, and processing performance, high damping, electromagnetic shielding, resourcefulness, easy recycling, and other advantages [14–17].

In this paper, for the thermal control design of the microsatellite, the lightweight material MB15 magnesium alloy is used as the main structure of the satellite. According to the structural layout of the satellite, the thermal characteristics of the stand-alone equipment, and the analysis of the in-orbit mission, the thermal design and analysis of the satellite are carried out. Active temperature control is adopted as the main focus, and through the modeling and calculation of the thermal analysis software Thermal Desktop-6.0, the stand-alone equipment's operating temperature is obtained for several working conditions. The working temperature of single equipment under several working conditions is obtained, which meets the design requirements. Through the heat balance test after the satellite assembly, the reliability of the thermal design is verified, which shows the rationality of the magnesium alloy MB15 used in the satellite structure design.

2. Microsatellite Design

2.1. Satellite Structural Design

The weight of the microsatellite is 30 kg, and its structure consists of 6 magnesium alloy structural panels. Satellite main load for the two-occultation antenna, distributed in the $\pm X$ structure plate, the satellite equipment is mainly divided into measurement and control communications, energy, attitude control, integrated electronics, and payload system of several major subsystems, the satellite layout is shown in Figure 1, the figure is only labeled with part of the single equipment code.

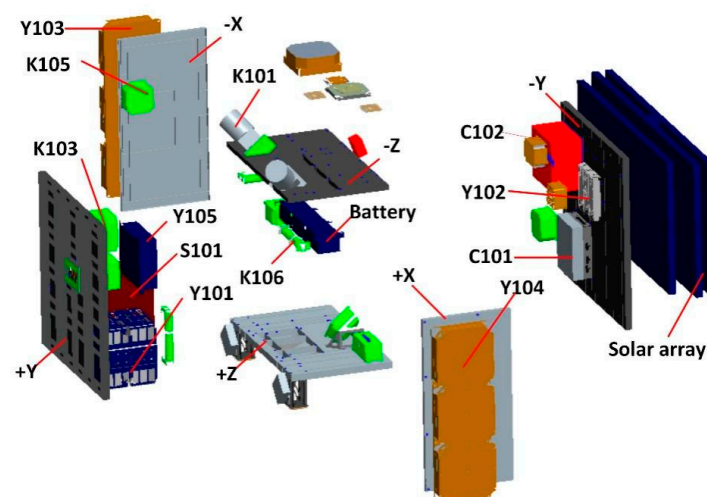


Figure 1. Satellite structure layout.

2.2. Thermal Control Indicator

The task of the thermal control subsystem is to take the necessary thermal control measures according to the satellite's orbit, attitude, configuration, equipment layout and heat consumption, working mode, environmental conditions, etc., in order to ensure that the on-board equipment maintains its work within the specified temperature range during

the entire mission period, thus ensuring the successful completion of the satellite's various tasks during the on-orbit flight.

There are many pieces of equipment on the satellite, and only some of the main equipment's thermal characteristics are listed here, as shown in Table 1.

Table 1. Main equipment thermal control indicators (°C).

Equipment Code	Equipment	Operating Temperature Requirements (°C)	Starting Temperature Requirements (°C)	Storage Temperature Requirements (°C)	Power Consumption (W)
S101	Avionics	−20~+50	−20~+50	−20~+50	10~16
C101	Regional Short Message Communication	−20~+50	−20~+50	−40~+85	2
C102	Telecontrol telemetry and data transmission test equipment	−20~+50	−20~+50	−40~+85	6
K101	Astrometer	−20~+50	−30~+60	−30~+60	0.8
K103	Fiber-optic gyroscopes	−20~+45	−40~+60	−40~+60	2.4
K105	Momentum wheel	−15~+50	−15~+50	−30~+60	0.8
K106	Magnetorquer	−15~+50	−15~+50	−30~+60	0.5
Y101	Occultation receiver	−15~+45	−15~+45	−20~+50	13
Y102	Preamplifier module	−15~+45	−15~+45	−20~+50	0.8
Y103	Occultation antenna 1	−90~+90	−90~+90	−90~+90	0
Y104	Occultation antenna 2	−90~+90	−90~+90	−90~+90	0
Y105	AIS load terminals	−20~+50	−20~+50	−40~+85	8

2.3. Magnesium Alloys Advantage

Micro-satellite structure plates using MB15 magnesium alloy material, which are designed in the form of skin and reinforcement, can not only ensure structural strength but also effectively reduce the structure's weight and lower the cost of launching. The magnesium alloy structure is designed to weigh 3.5 kg, which is one-third lighter than the aluminum alloy structure under the same structure design. In order to be able to accurately perform thermal analysis of the satellite, we used MB15 magnesium alloy for the physical properties of the detection of the state. The satellite structure plate state is consistent with the surface of the native color conductive oxidation, the test results are compared with the 2A12 aluminum alloy and shown in the Table 2.

Table 2. MB15 magnesium alloy parameters.

Testing Program	MB15 Magnesium Alloys	2A12 Aluminum Alloy
25 °C thermal conductivity W/(m·K)	94.8	130
specific heat capacity J/(kg·K)	1010	921
solar absorption ratio	0.40	0.2
hemispheric emissivity	0.05	0.3

3. External Heat Flow Analysis

The external heat flow to which a satellite is subjected in orbit mainly consists of three parts: solar radiation, Earth albedo, and Earth infrared [9,18,19], as shown in Figure 2. Among them, the Earth infrared is only related to the orbital altitude. It does not change much during the life cycle, so the changes in the external heat flow in space are mainly reflected in the changes in solar radiation and Earth albedo, which are due to the cyclic motion of the sun in the ecliptic plane, resulting in the continuous change in the angle between the sunlight vector and the satellite orbital plane within a certain range [20–22].

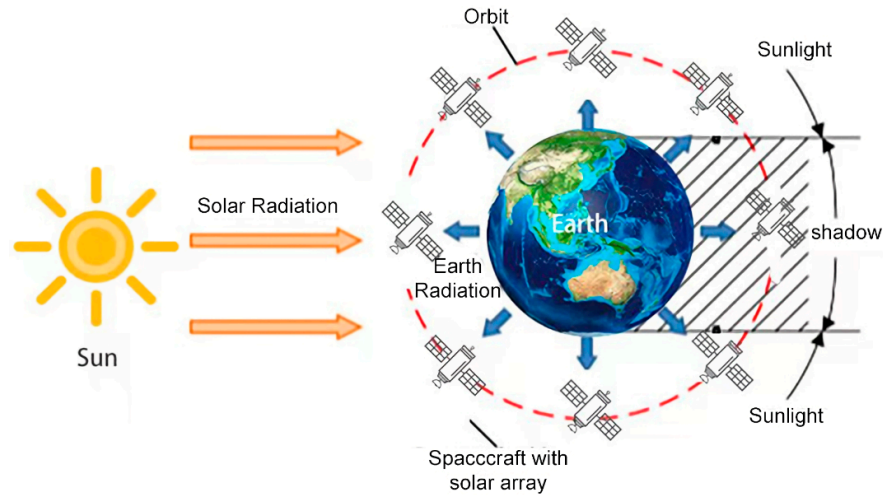


Figure 2. In-orbit thermal environments.

The satellite operates in a sun-synchronous orbit with an orbital altitude of 500 km, an orbital inclination of 97.4° , and a descending node local time of 6:00 a.m. According to its orbital type and parameters, its orbital year-round β -angle can be derived by using the STK-9.2 software as shown in Figure 3. β_{max} and β_{min} have maximum β -angles of 87° , which corresponds to the date of March 2, and minimum β -angles of 59° , which corresponds to June. The minimum β angle is 59° , which corresponds to June 21st. The β -angle is the angle between the sunlight vector and the satellite orbital plane, which is a crucial design parameter in the thermal control design of satellites and is closely related not only to the density of the sunlight heat flow arriving at the surface of the satellite but also to the density of the Earth’s reflected heat flow arriving at the surface of the satellite.

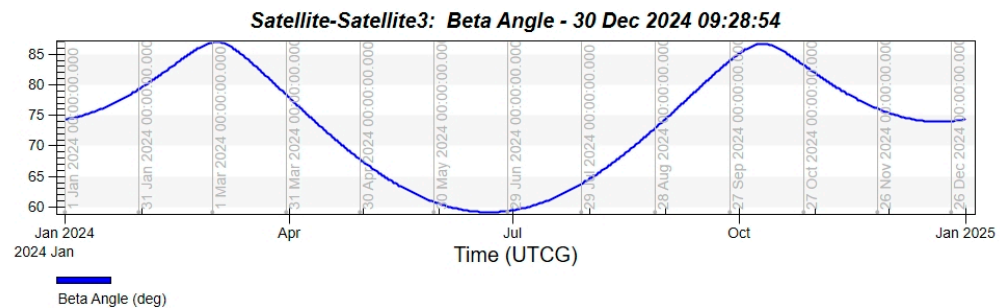


Figure 3. β -angle change curve.

When the satellite is in orbit, the two cases of β -angle, 87.0° and 59° , are taken for the external heat flow analysis, and the external heat flow of each surface of the load in one orbital cycle under two β -angles is calculated and obtained, as shown in the following Figure 4.

In order to obtain a more intuitive understanding of the external heat flow to which the satellite is subjected while in orbit, the average external heat flow of each surface at different β -angles is counted, as shown in Table 3.

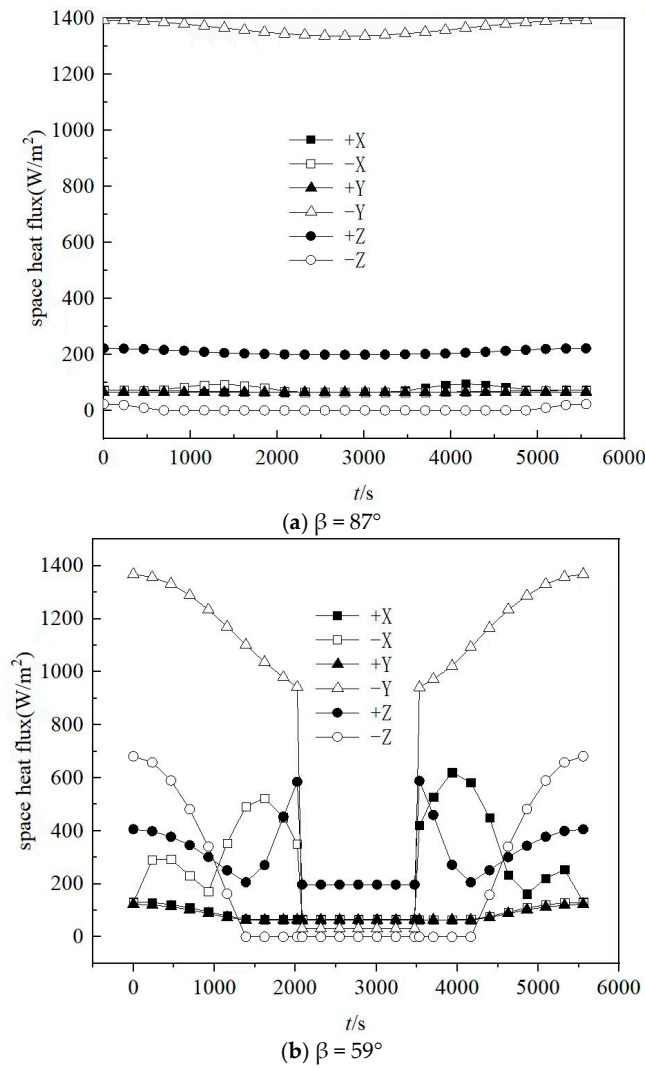


Figure 4. Variation curves of the external heat flux from each satellite surface at an orbital altitude of 500 km.

Table 3. Mean arrival outside heat flow at surfaces with different β -angles (W/m^2).

Different Structural Plates	500 km					
	$\beta = 87^\circ$			$\beta = 59^\circ$		
	Solar Radiation (W/m^2)	Earth Reflection (W/m^2)	Earth Infrared (W/m^2)	Solar Radiation (W/m^2)	Earth Reflection (W/m^2)	Earth Infrared (W/m^2)
+X	4.5	4.4	59.6	102.6	20.3	59.0
-X	4.4	4.4	58.7	102.6	20.4	60.5
+Y	0.0	0.2	57.6	0.0	15.5	60.2
-Y	1336.4	7.7	28.4	863.2	13.0	28.2
+Z	0.0	13.4	192.6	49.8	65.7	192.8
-Z	3.4	0.0	0.0	215.2	0.0	0.0

From the above figures and tables, the +Y surface is not irradiated by the sun under the normal attitude of the satellite, and the Earth albedo and infrared are also smaller and very stable, which makes it suitable as the main heat dissipation surface of the whole satellite. The -Y surface is exposed to the sun for an extended time, and the average external heat flow is the largest, so it is not suitable for the heat dissipation surface. The external heat flow of the $\pm X$ surface varies significantly in each cycle, so it is generally not used as the main heat dissipation surface but can instead be used as the auxiliary heat dissipation surface of the single equipment on the satellite. The -Z surface faces away from the Earth,

meaning there is no Earth albedo or infrared. However, the illumination time is extensive, the sun is directly irradiated by the most significant change in external heat flow, and the total level of heat flow is not high. Under tight conditions, this can be used as an auxiliary heat dissipation surface of the satellite. Because the +Z surface is always to the Earth, the Earth albedo and Earth infrared are relatively large. It is less efficient for use as a heat dissipation surface, but the fluctuation of the external heat flow is small, so according to the equipment layout, it can be considered an auxiliary heat dissipation surface.

4. Satellite Thermal Design Program

The satellite thermal control design should inherit the flight-verified design means and select thermal control components undergoing long-term on-orbit flight verification. It adopts the control mode of passive thermal control, mainly supplemented by electric heating as an active control. And according to the satellite's short orbital period, the instrument power fluctuation changes significantly, carrying out transient thermal design analysis and test work to improve the reliability of the thermal design scheme. In addition, specialized thermal designs or tests are carried out for equipment or components with special requirements for temperature control, such as lithium-ion batteries.

The thermal control system not only needs to maintain the satellite's stand-alone equipment within its specified temperature range but also provide sufficient heat dissipation for electronic equipment that consumes large amounts of power and works for long periods of time. In order to achieve this goal, the thermal control system of the microsatellite adopts a combination of passive and active thermal control methods to carry out a detailed thermal design for each component, and the Table 4 shows the thermal consumption of the main equipment in each operating mode of the whole satellite.

Table 4. Satellite heat consumption in different operating modes.

Equipment	Damping Stage (W)	Load On (W)	Orbit Control Mode (W)
C101	2	2	2
C102	6	6	6
K101	0.8	0.8	0.8
K103	2.4	2.4	2.4
K105	0	0.8	0.8
K106	0.5	0.5	0.5
S101	10	16	16
Y101	0	13	0
Y102	0	0.8	0
Y103/Y104	0	0	0
Y105	0	8	0

4.1. Thermal Design

According to the external heat flow characteristics and equipment layout, the +Y board is used as the heat dissipation surface, as shown in Figure 5. The inner surface of the heat dissipation surface is sprayed with E51-M black paint, and the outer surface is sprayed with SR107-ZK white paint. In addition to the lithium battery temperature control range being narrower, the temperature control requirements of other equipment in the satellite are closer, so in addition to the lithium battery, the surface of other structures and equipment in the satellite are treated with high emissivity to strengthen the radiative heat transfer between the equipment in the satellite and between the equipment and the heat sink surface, which is conducive to the dissipation of heat from the equipment. The satellite's high heat-consuming equipment and the mounting surface between the coating of thermal grease, in order to reduce the contact thermal resistance, strengthen the heat transfer. For equipment exposed outside the cabin, its surface is treated by cladding multi-layer heat-insulating components, spraying white paint, pasting F46 film or gold plating, etc., to reduce the

temperature fluctuation caused by changes in the external heat flow, and at the same time, active electric heating is utilized to improve the temperature level of the equipment.

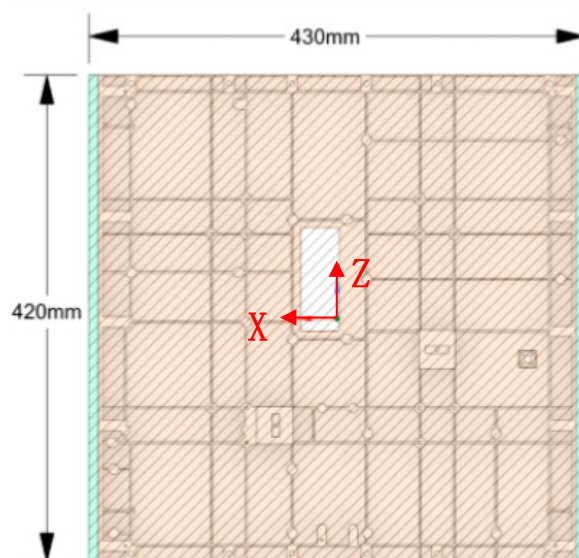


Figure 5. Schematic diagram of heat dissipation surface.

Thermal Desktop 6.0 software was used to establish the thermal analysis model of the satellite; the satellite model is divided into 7201 nodes, and the thermal analysis model is shown in Figure 6.

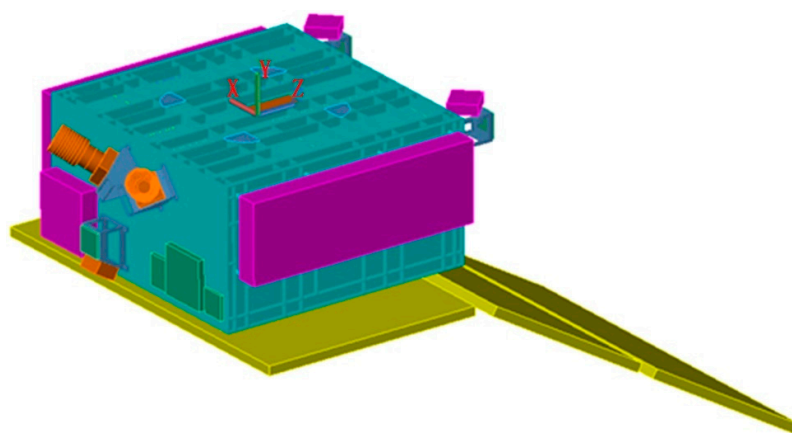


Figure 6. Thermal analysis model.

The following simplifications were used for modeling:

- (a) The sunlight is considered parallel, i.e., the sunlight diffusion angle is 0.
- (b) Specular reflection between surfaces is not considered. Each surface is treated as a gray body, and surface radiation satisfies Lambert's law.
- (c) The internal heat transfer of the main heat-generating part of the equipment is not considered, and the main heat-generating part of the equipment is reduced to an isothermal body.
- (d) The equipment mounting bracket is simplified to ensure the heat transfer relationship, ignoring rounding and chamfering.

Thermal Control of Special Equipment

Battery: Due to the narrow temperature control range of lithium batteries, in order to reduce the impact of the cabin cooling surface and equipment temperature fluctuations on the lithium battery, the battery shell surface is wrapped with 5 units of multilayer insulation components, the membrane using double-sided aluminized polyester film. Battery mounting surface pad a layer of polyimide film to meet the requirements of the single secondary insulation. Battery set up one main and one backup 2-way temperature control circuit.

Propulsion: Thrusters and bulkheads are thermally insulated. The thrusters are mounted on the bottom plate with a low absorption-to-emission ratio treatment to reduce the absorbed external heat flow and to dissipate the waste heat from the electric propulsion operation to the cold space. The rest of the surface is treated with a high emissivity treatment.

Star-tracker: 1, star-tracker body wrapped in 15 units of multi-layer thermal insulation components, mask for the yellow film; 2, star-tracker bracket cabin outer part of the surface wrapped in 15 units of multi-layer thermal insulation components, mask for the yellow film, bracket cabin part of the black treatment; 3, star-tracker and the bracket, the bracket and the cabin plate are thermally conductive between the mounting, the contact surface is coated with thermally conductive silicone grease;

Digital Taemin: In addition to the mounting surface and $-Z$ surface, all other surfaces are wrapped with a multi-layer thermal insulation assembly with an F46 film; $-Z$ surface, in addition to the light-entry port, is pasted with an F46 film; 3. Taemin is mounted with a heat-conducting bulkhead.

4.2. Thermal Analysis Results

According to the external heat flow analysis results based on the characteristics of the thermal control program, this study only selected three typical working conditions. It was found that the satellite equipment was too expensive, so this paper only selected some of the main stand-alone equipment thermal analysis results, which can be seen in the Table 5.

Table 5. Simulation analysis results.

Equipment	Security Mode °C	Load-On Mode °C	Safe Mode °C	Working Temperature °C
C101	−0.7~2	21.1~23.1	20.9~25.3	−20~50
C102	9~12.4	31.9~34.5	29.9~33.9	−20~50
K101	7.6~14	25.8~31.5	24.5~31.5	−30~40
K103	8.2~11.8	35.7~38	26.8~33.0	−20~45
K105	0.3~2.9	28.5~30.1	27.1~32.3	−15~50
K106	19.2~21	36.9~38.8	36.9~39.2	−15~50
S101	−2.3~0.6	23.1~26.8	21.5~26	−20~50
Y101	−5.3~−3.3	25.3~26.2	20.4~24.9	−15~45
Y102	−3.4~−1.2	21.8~22.9	19.8~24.9	−15~45
Y103	−42.7~−34.2	−32.8~5.3	−11.9~87.2	−90~90
Y104	−40.1~−31.2	−34.7~7.6	−39.1~−22.2	−90~90
Y105	5.1~8.3	34.5~36	23.7~35.1	−90~90

Working condition 1 is a safe mode; in this mode, the platform equipment (platform equipment is primarily equipment other than the load equipment) is turned on for a long time (momentum wheel off); occultation and AIS load off digital transmission are not turned on; propulsion is not turned on, and the satellite attitude is lost. We need to consider each face to the sun, along the axis of spinning along the sun; this stage of the temperature level should be emphasized for analysis, especially for a certain direction to the sun. The satellite will be utilized in the mode of high and low temperatures. The cloud

diagram of the operating temperature of the equipment under this condition is shown in Figure 7.

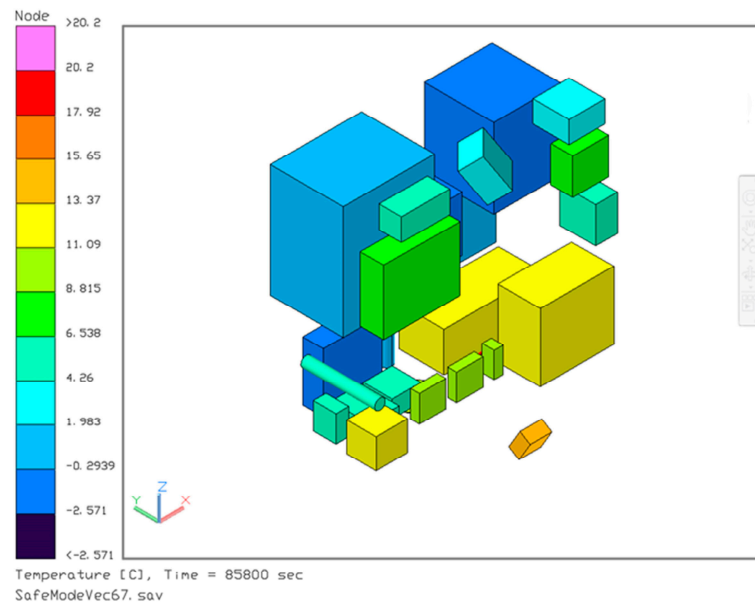


Figure 7. Equipment temperature cloud in security mode.

Condition 2 is the high-temperature mode of load start-up. When the load is started, the satellite temperature reaches the cycle of stable equilibrium. This occurs when the temperature distribution of each device and instrument, after turning on the active thermal control, ensures that the power-on equipment is within its working temperature range, as well as when the non-power-on equipment (propulsion, AIS load terminator, occultation receiver, and the preamplifier module) is within the range of its working/startup/storage temperature. There is a certain temperature margin, and the equipment temperatures meet the target requirements. Currently, the average power consumption for battery active thermal control power per track is 3.4 W. The cloud diagram of the operating temperature of the equipment under this condition is shown in Figure 8.

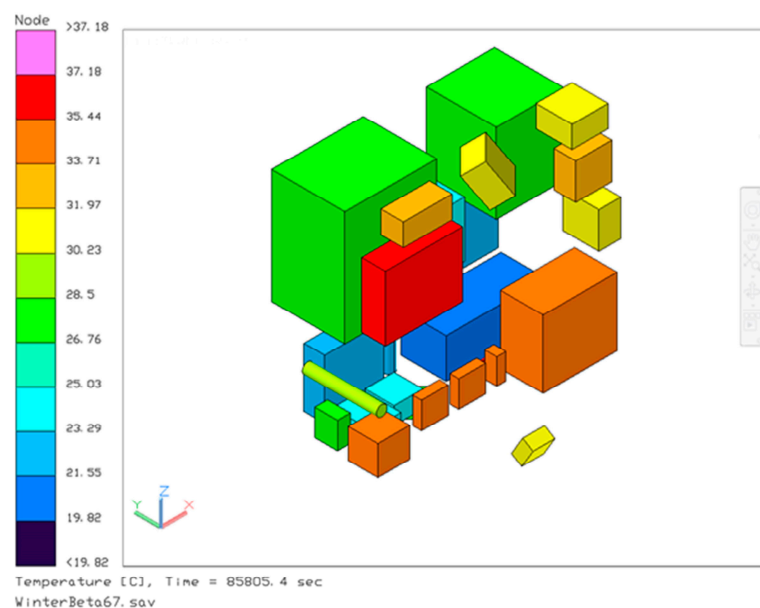


Figure 8. Equipment temperature cloud in load-on mode.

Condition 3 is the orbit control mode, which calculates the temperature distribution of each equipment and instrument on the satellite under high-temperature working conditions; when the satellite is in orbit control mode, and the electric push is on, the temperature distribution of the main equipment on the satellite is shown in Table 5. From the temperature recalculation results in the table, it can be seen that $\beta = 67^\circ$, all the equipment is in the range of their working temperatures. The equipment not turned on is in the range of their working/starting/storage temperatures, and there is a certain temperature margin, and all the equipment temperatures meet the target requirements. The temperature of the equipment meets the requirements of the index. The cloud diagram of the operating temperature of the equipment under this condition is shown in Figure 9.

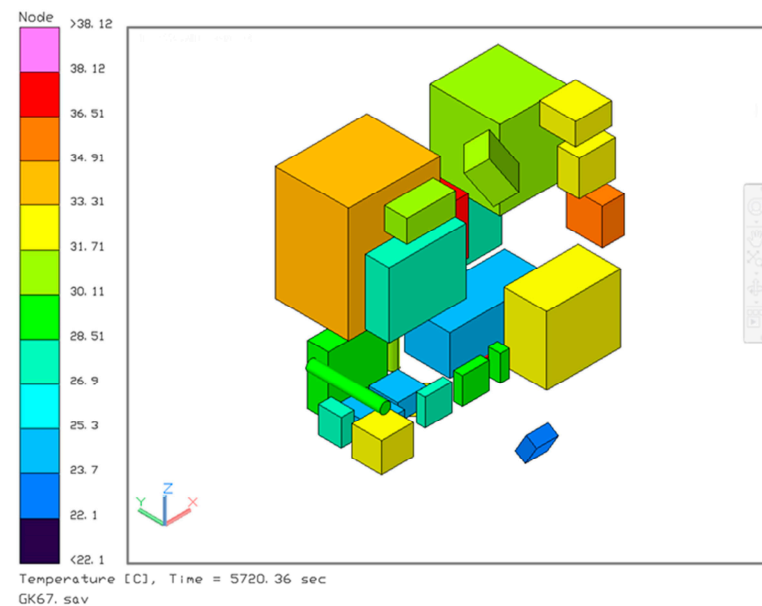


Figure 9. Equipment temperature cloud in orbit control mode.

5. Thermal Balance Test

At present, it is not possible to solve the spacecraft thermal design problem by means of thermal simulation alone, and thermal balance tests must be conducted to verify the correctness of the thermal design. The thermal balance test is a supplement to and verification of the thermal analysis, and it is necessary to carry out the thermal balance test to obtain the temperature distribution data under the working condition of the main equipment of the satellite and establish an accurate thermal model.

5.1. Test Program

There are two thermal vacuum tests: the thermal balance test and the acceptance-level thermal vacuum test. The purpose of the thermal balance test is to obtain satellite temperature distribution data, assess the ability of the thermal control subsystem to maintain on-board equipment within the specified temperature range, thereby verifying the correctness of the thermal design, and at the same time, provide a basis for setting the test temperature for the acceptance-level thermal vacuum test. The purpose of the thermal vacuum test is to expose potential quality defects in the satellite's materials, processes, and manufacturing under the prescribed vacuum pressure and acceptance-level thermal cycling stress and to verify the reliability of the satellite's work in a thermal vacuum environment.

In the thermal balance test, the key to obtaining accurate temperature results is to accurately simulate the heat flow outside the satellite orbit, and at present, the main ways of simulating the external heat flow are a solar simulator, infrared light array, heating sheet,

and infrared heating cage. In the satellite thermal balance test, the infrared heating cage has the characteristics of low cost, accurate heat flow simulation, and adaptable parameter design with the demand of heat flow simulation, and the infrared cage is more suitable for solving the problem of simulating the heat flow on the surface of microsattellites. Its characteristics are more in line with the requirements of the low-cost test of microsattellites.

During the thermal balance test of the satellite, the vacuum tank is used to simulate the space environment, and the infrared cage is used to simulate the external heat flow absorbed by the payload. Figure 10 shows the physical diagram of the heat balance test of the micro-satellite, including the satellite, the infrared cage, and the vacuum tank.

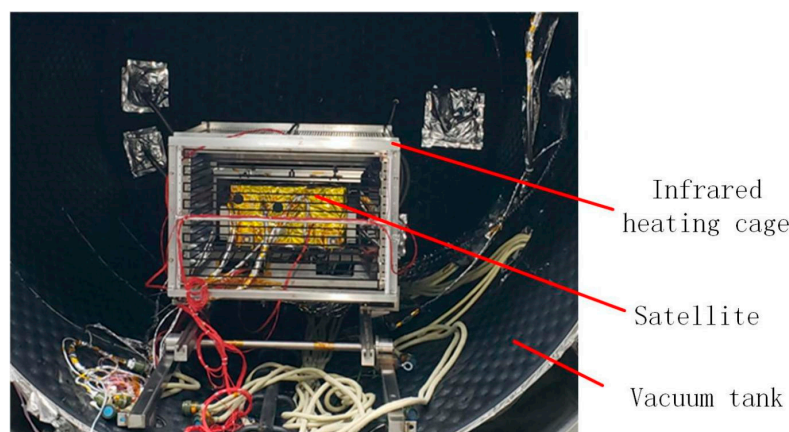


Figure 10. Physical drawing of thermal balance test.

5.2. Test Conditions

According to the external heat flow to which the microsatellite is subjected, the working mode, the internal heat source distribution, and the thermophysical state of the thermal control coating, 2 extreme working conditions are planned, and the specific settings are shown in Table 6. To make the test data more representative, we only extracted the worst two working conditions to list the comparison.

Table 6. Thermally balanced condition.

Condition		Main Setting Conditions
Case 1	Thermally balanced low-temperature condition	The β -angle is taken as 87.0° , and the solar constant is taken as 1322 W/m^2 ; the multi-layer surface is F46 film, and the performance parameter is $\alpha_s/\varepsilon = 0.15/0.69$; the surface of the heat sink surface is SR107–ZK white lacquer, and the performance parameter is $\alpha_s/\varepsilon = 0.17/0.87$; the active thermal control works.
Case 2	Thermally balanced high-temperature condition	The β -angle is taken as 59° , and the solar constant is taken as 1414 W/m^2 ; the multilayer surface is F46 film with the performance parameter $\alpha_s/\varepsilon = 0.36/0.69$; the surface of the heat sink surface is SR107–ZK white lacquer, and the performance parameter is $\alpha_s/\varepsilon = 0.4/0.87$; and the active thermal control works.

5.3. Test Results and Analysis

According to the designed working conditions, the heat balance test was completed from low to high temperatures. Each device is a single-point temperature measurement carried out by means of a thermistor with a temperature deviation of no more than $0.3 \text{ }^\circ\text{C}$. The thermal equilibrium low temperature is shown in Case 1; the thermal equilibrium high temperature is shown in Case 2; Circle I represents thermal vacuum cycle I; and Circle II represents thermal vacuum cycle II. The vacuum degree during the thermal equilibrium test

is 3.7×10^{-5} Pa, and the heat sinking temperature is 90 K. According to the test results, the temperature curves of some key components in different working conditions are plotted, as shown in Figures 11 and 12.

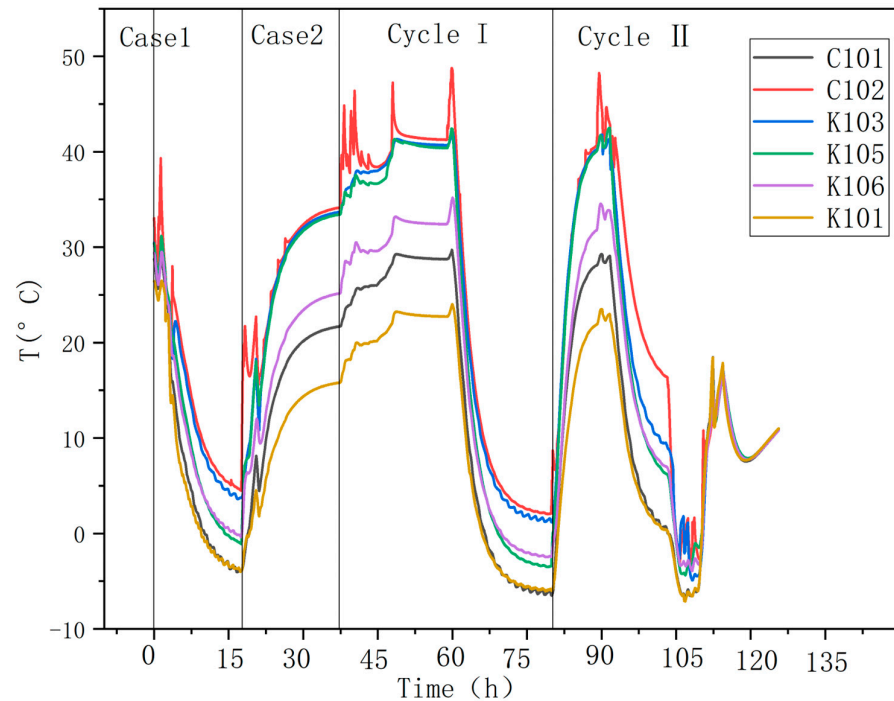


Figure 11. Temperature profile of some equipment.

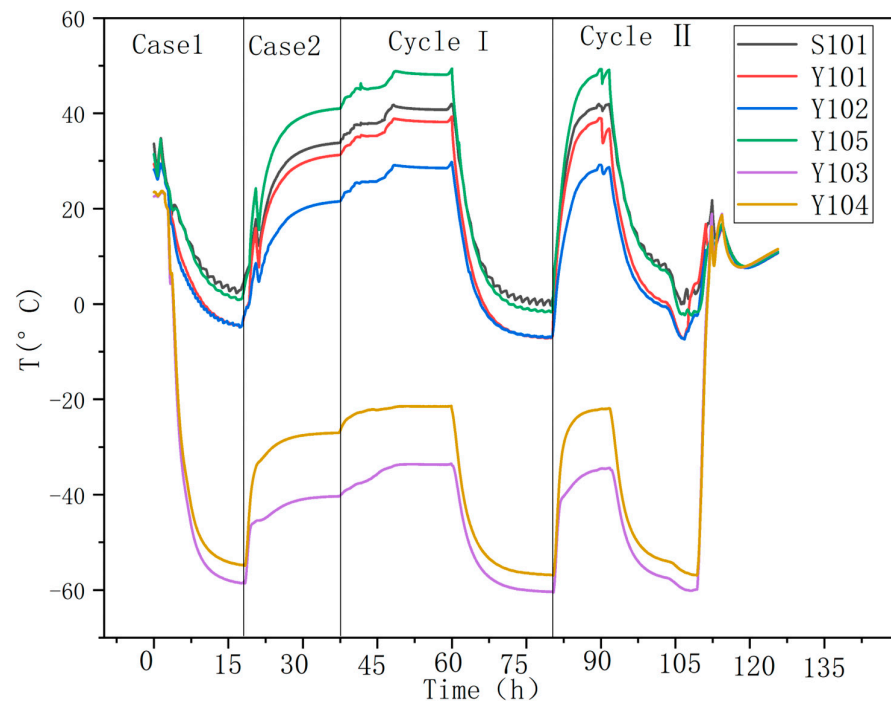


Figure 12. Temperature profile of some some main equipment.

The temperature data of key components under heat balanced high-temperature operating conditions and low heat balance temperature operating conditions were compiled based on the test results, as shown in Table 7.

Table 7. Temperature of critical equipment (°C).

Equipment	Case 1	Case 2	Thermal Control Indicators	Deviation Between Test and Simulation Data	
				Case 1	Case 2
C101	−3.94	21.64	−20~50	0.26	−0.23
C102	4.55	34.08	20~50	1.19	0.4
K101	−3.52	16.5	30~40	0.45	0.46
K103	3.75	33.64	−20~45	0.64	0.42
K105	−1.05	33.36	−15~50	0.12	0.38
K106	−0.30	25.10	−15~50	0.1	0.15
S101	2.94	33.72	20~50	0.23	−0.25
Y101	−4.71	31.2	15~45	−0.82	−0.59
Y102	−4.84	21.46	−15~45	−1.61	−1.63
Y103	−58.52	−40.35	−90~90	−0.28	−0.42
Y104	−54.7	−27.03	−90~90	−0.32	−0.36
Y105	0.96	40.92	20~50	0.12	0.13

As can be seen from Figures 8 and 9 and Table 5, the temperature of each heating zone in the two typical working conditions can be controlled near the target temperature, indicating that the active heating zone is reasonably designed; the temperature of the heat source in the load cell is normal, indicating that the heat sink can effectively dissipate heat, and the heat dissipation path is normal. The deviation between the temperature of the thermistor and thermocouple at the same moment in the thermal analysis simulation data and thermal balance test is generally within 0.5 °C, and the maximum difference is not more than 1.7 °C, which indicates that the simulation model is well established, and the thermal analysis is reliable. At the same time, the temperature of the stand-alone equipment in the thermal simulation and thermal experiment state is within the temperature requirement range, proving that the thermal design is reasonable and feasible.

6. Conclusions

In this paper, according to the lightweight demand of the structure of the microsatellite, MB15 magnesium alloy is used in the satellite structural plate, and the weight of the structure is reduced by one-third. The MB15 magnesium alloy used is tested for thermal physical properties, and a detailed thermal design of its thermal control system is carried out according to the space environment, structural characteristics, and working mode of the satellite. The thermal design process mainly adopts passive thermal control measures such as multi-layer heat-insulating components, white paint, black paint, heat-insulating pads, heat-conducting fillers, and blackening treatment for heat insulation, heat conduction, and heat dissipation; at the same time, it adopts active thermal control measures such as electric heaters for temperature compensation. Through simulation analysis, the temperature of each equipment is within the required range, indicating that the thermal design is reasonable.

In order to verify the correctness of the thermal design, a thermal balance test was conducted on the satellite according to the planned extreme working conditions. The results of the thermal balance test show that the temperature of every single piece of equipment of the satellite meets the requirements under different working conditions, which is close to the results of the simulation analysis, verifying the reliability of the thermal analysis and the rationality of the thermal design of the whole satellite. The simulation and test also proved that the application of magnesium alloy in the structure of the microsatellite is feasible, reducing the weight of the structure, but also through the thermal design to meet the requirements of the thermal control indices of the single equipment on the satellite, which adds a new choice for the subsequent selection of materials for microsatellites.

Author Contributions: Investigation, H.H.; Data curation, C.B.; Writing—review & editing, H.H.; Supervision, C.B. All authors have read and agreed to the published version of the manuscript.

Funding: This research received no external funding.

Data Availability Statement: The data presented in this study are available on request from the corresponding author. The data are not publicly available due to privacy.

Conflicts of Interest: The authors declare no conflict of interest.

References

1. Frisch, H.P. Thermally induced vibrations of long thin-walled cylinders of open section. *J. Spacecr. Rocket.* **1970**, *7*, 897–905. [[CrossRef](#)]
2. Chen, J.; Zhang, X.; Chen, W.D. Research on design of low mass structure for a minisatellite. *J. Aerosp. Shanghai* **2014**, *31*, 30–35.
3. Corpino, S.; Caldera, M.; Nichele, F.; Masoero, M.; Viola, N. Thermal design and analysis of a nanosatellite in low earth orbit. *J. Acta Astronaut.* **2015**, *115*, 247–261. [[CrossRef](#)]
4. Yoo, J.G.; Jin, H.; Seon, J.H.; Jeong, Y.H.; Glaser, D.; Lee, D.H.; Lin, R.P. Thermal Analysis of TRIO-CINEMA Mission. *J. Astron. Space Sci.* **2012**, *29*, 23–31. [[CrossRef](#)]
5. Daeil, P.; Kikuko, M.; Hosei, N. Thermal design and validation of radiation detector for the ChubuSat-2 micro-satellite with high-thermal-conductive graphite sheets. *Acta Astronaut.* **2017**, *136*, 387–394.
6. Li, S.J.; Chen, L.H.; Liu, S. Thermal analysis model correction method based on Latin hypercube sampling and coordinate rotation method. *J. Therm. Stress.* **2023**, *46*, 857–870. [[CrossRef](#)]
7. Zhao, X. Applications of magnesium alloys at aluminum honeycomb sandwich structure panel. *J. Aerosp. Mater. Technol.* **2008**, *4*, 48–50.
8. Phoenix, A.A. Variable Thermal Conductivity Metamaterials Applied to Passive Thermal Control of Satellites. *J. Thermal Sci. Eng. Appl.* **2023**, *15*, 121007. [[CrossRef](#)]
9. Atar, C.; Aktaş, M.; Sözbir, N.; Bulut, M. Analytical Investigation of Surface Temperatures for Different Sized CubeSats at Varying Low Earth Orbits. *J. Thermal Sci. Eng. Appl.* **2023**, *15*, 081002. [[CrossRef](#)]
10. Xie, G.; Liu, Y.; Sunden, B.; Zhang, W. Computational Study and Optimization of Laminar Heat Transfer and Pressure Loss of Double-Layer Microchannels for Chip Liquid Cooling. *J. Thermal Sci. Eng. Appl.* **2013**, *5*, 011004. [[CrossRef](#)]
11. Sairajan, K.K.; Nair, P.S. Design of low mass dimensionally stable composite base structure for a spacecraft. *J. Compos. Part B-Eng.* **2011**, *42*, 280–288. [[CrossRef](#)]
12. Cho, H.K. Maximizing structure performances of a sandwich panel with hybrid composite skins using particle swarm optimization algorithm. *J. Mech. Sci. Technol.* **2009**, *23*, 3143–3152. [[CrossRef](#)]
13. Du, Z.; Zhu, M.; Wang, Z.; Yang, J. Design and application of composite platform with extreme low thermal deformation for satellite. *J. Compos. Struct.* **2016**, *152*, 693–703.
14. Xiao, G.; Du, Y.; Gui, Y.; Liu, L.; Yang, X.; Wei, D. Heat transfer characteristics and limitations analysis of heat-pipe cooled thermal protection structure. *Appl. Therm. Eng.* **2014**, *70*, 655–664.
15. Tang, H.; Lian, L.; Zhang, J.; Liu, Y. Heat transfer performance of cylindrical heat pipes with axially graded wick at anti-gravity orientations. *Appl. Therm. Eng.* **2019**, *163*, 114413. [[CrossRef](#)]
16. Xia, L. The General Optimization of Dynamic Characteristics for Satellite Structure. Ph.D. Thesis, Shanghai Communication University, Shanghai, China, 2002. (In Chinese).
17. Thornton, E.A.; Paul, D.B. Thermal-structural analysis of large space structures: An assessment of recent advances. *J. Spacecr. Rocket.* **1985**, *22*, 385–393. [[CrossRef](#)]
18. Yang, Z.; Li, J.; Zhang, J.X.; Lorimer, G.W.; Robson, J.A.M.S.E.L. Review on research and development of magnesium alloys. *J. Acta Metall. Sin.* **2008**, *21*, 313–328. [[CrossRef](#)]
19. Asim, M.; Azhar, M.; Moeenuddin, G.; Farooq, M. Correcting solar radiation from reanalysis and analysis datasets with systematic and seasonal variations. *J. Case Stud. Therm. Eng.* **2021**, *25*, 221–235.
20. Johnston, J.D.; Thornton, E.A. Thermally induced dynamics of satellite solar panels. *J. Spacecr. Rocket.* **2000**, *37*, 604–613. [[CrossRef](#)]
21. Behrooz, H.; Karimian, S.M.H. Determining the heat flux absorbed by satellite surfaces with temperature data. *J. Mech. Sci. Technol.* **2014**, *28*, 35–46.
22. Li, J.; Yan, S.; Cai, R. Thermal analysis of composite solar array subjected to space heat flux. *J. Aerosp. Sci. Technol.* **2013**, *27*, 84–94. [[CrossRef](#)]

Disclaimer/Publisher’s Note: The statements, opinions and data contained in all publications are solely those of the individual author(s) and contributor(s) and not of MDPI and/or the editor(s). MDPI and/or the editor(s) disclaim responsibility for any injury to people or property resulting from any ideas, methods, instructions or products referred to in the content.